Use of Alternative Alkali-Activated Mortars for Textile Reinforced Mortar Systems

Use of alternative alkali-activated mortars for Textile Reinforced Mortar systems

Jacopo Donnini[1*], Alessandra Mobili[1], Francesca Tittarelli[1], Valeria Corinaldesi[1]

[1] Dep. of Science and Engineering of Matter, Environment and Urban Planning-SIMAU, Università Politecnica delle Marche, Ancona, Italy

[*]jacopo.donnini@staff.univpm.it

Abstract. The need for repair and strengthening existing buildings has become fundamental in the construction sector. At the same time, the efforts to reduce global CO_2 emissions are leading to the development of building materials with low environmental impact, such as those based on alkali-activated mortars (AAMs). When compared to traditional mortars, AAMs allow to reduce CO_2 emissions in a range from 30% to 80%. Recent studies have demonstrated the possibility of using AAMs as alternative matrices for structural strengthening systems, such as Textile Reinforced Mortar (TRM).
This study evaluates the possibility of using different formulations of AAMs, based on metakaolin or fly ash, for TRM applications. The newly developed TRMs are compared in terms of physical and mechanical performances with two commercially available TRMs, based on lime or cementitious mortars. A bidirectional basalt fabric was used as internal reinforcement. The effectiveness of these new systems, also referred to as Textile Reinforced Alkali-Activated Mortars (TRAAMs), has been evaluated through direct tensile tests on prismatic coupons and shear bond tests on clay brick substrates. Experimental results showed that AAMs can be very promising as sustainable alternative to traditional mortars for TRM systems.

Keywords: TRM, alkali-activated mortar, geopolymer, strengthening, fibers.

1 Introduction

Nowadays, the use of Textile Reinforced Mortar (TRM), also called Fabric-Reinforced Cementitious Matrix (FRCM), for strengthening and rehabilitation of existing masonry and concrete structures has become a well-established technique [1]. This system presents several advantages if compared to traditional reinforcement techniques (steel or concrete jacketing, FRPs) such as low invasiveness, lightness, ease of application, possibility of application on wet surfaces, high durability and reversibility. The internal fabric is usually a bidirectional grid made of carbon, basalt, glass or PBO fibers [2,3]. The inorganic matrix is a cement- or lime-based mortar. The former is preferred for the strengthening of concrete structures while the latter is more suitable for masonry, especially in the case of cultural heritage architectures.

In recent years, there has been increasing interest in evaluating the possible use of matrices with a lower environmental impact, such as those based on alkali-activated

mortars (AAMs) [4,5]. In addition to having a lower carbon footprint, compared to cement- or lime-based mortars [6], AAMs also possess interesting properties such as better fire resistance [7], high mechanical properties and durability in aggressive environments [8]. In this study, the possibility of using AAMs, based on fly ash or metakaolin, for TRM applications, has been preliminary evaluated. Mortars have been firstly characterized in terms of mechanical properties. Then, their potential utilization in TRAAM systems has been evaluated through uniaxial tensile tests and single-shear bond tests on clay brick substrates. Performances of TRAAM systems have been discussed and compared to those of commercial lime- and cement-based TRM systems.

2 Materials

2.1 Mortars

Four different mortars have been characterized and tested. The first two are AAMs, based on fly ash (FAK) or metakaolin (MKK), while the others are commercially available mortars based on lime or cement. MKK and FAK were designed in order to have physical and mechanical properties comparable to those of the lime-based and cementitious mortars, respectively. The alkaline solutions used are a blend of sodium silicate, potassium hydroxide and water. A calcareous sand with maximum diameter of 3 mm and water absorption of 3.4% by mass was used as aggregate. Mix proportions of AAMs are reported in Table 1.

Table 1. Mixture proportions of AAMs (kg/m^3).

Mortar	Sand	Mixing water	Fly ash	Calcium aluminate cement	Metakaolin	Sodium silicate	Potassium hydroxide	Water
FAK	1409	-	480	42	-	157	62	94
MKK	1090	44	-	-	404	242	65	178

2.2 Fabric

The fabric used as reinforcement for all TRM systems is a bidirectional basalt fabric pre-impregnated with a polyester coating. The spacing between yarns is about 20 mm and the cross-sectional area of a single yarn is 1.33 mm^2. The fabric has a net weight of 365 g/m^2 and a total weight (comprising the coating) of 420 g/m^2. The yarn tensile strength and elastic modulus (as reported by the manufacturer) are equal to 1402 MPa and 72 GPa, respectively.

3 Experiments and results

3.1 Characterization of mortars

Three prismatic specimens (40x40x160 mm^3) for each mortar were manufactured and cured at laboratory conditions (20 ± 2 °C, RH = 65 ± 5%). After 28 days they were tested according to the UNI EN 1015-11:2019 standard to evaluate compressive and flexural strength. The dynamic modulus of elasticity was also evaluated, according to the UNI EN 12504-4:2021 standard. Results are reported in Table 2.

Table 2. Properties of mortars

Mortar	Compressive strength (MPa)	Flexural strength (MPa)	Dynamic modulus of elasticity (GPa)
FAK	27.4	8.6	24.6
MKK	8.8	1.7	8.3
LIME	9.5	3.6	10.1
CEM	43.8	6.9	24.1

It is interesting to observe that FAK mortars showed the highest flexural strength, and a modulus of elasticity comparable to that of cementitious mortars (about 24 GPa). MKK mortars showed compressive strength and modulus of elasticity comparable to those of lime-based matrices, while the flexural strength is lower.

3.2 Tensile tests on TRM coupons

To evaluate the feasibility of using AAMs for TRM applications, and to compare their performances to those of commercial systems, a total of 16 prismatic coupons (60x380x10 mm^3) were manufactured by using a basalt fabric as internal reinforcement (Figs. 1a,b). The fabric was carefully placed between two layers of mortar, to form a composite with total thickness of 10 mm. Coupons were covered with a PVC film and cured for 28 days at laboratory conditions. Before testing, glass FRP tabs were epoxy glued at the ends of each specimen, to avoid slippage and premature failure during tensile tests.

Tests were performed in displacement control (0.5 mm/min) with a universal tensile testing machine with maximum capacity of 50 kN. A clamping grip system was used. Strain was measured using Digital Image Correlation (DIC) technology (Fig. 1c).

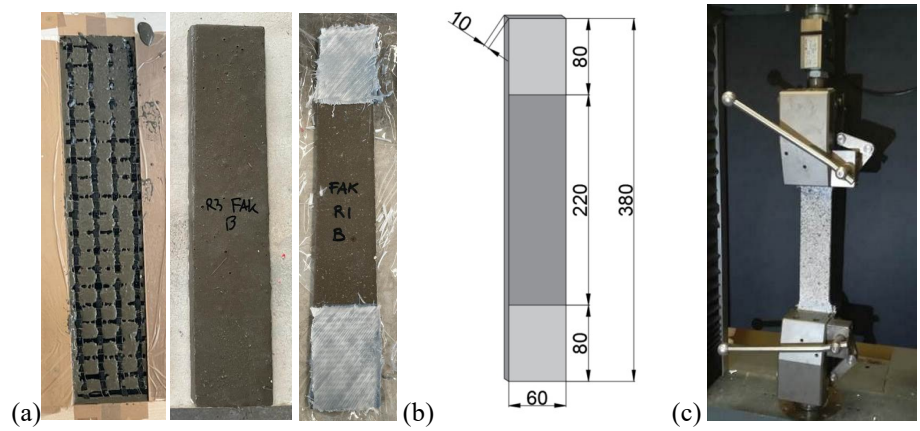

Fig. 1. Tensile test: (a) Specimens manufacturing, (b) TRM coupon geometry and (c) test setup.

Results of tensile tests are reported in Table 3. Tensile stress is calculated by dividing the tensile load by the cross-sectional area of the reinforcing basalt fabric. The tensile stress at first crack is reported as $\sigma_{t,1}$, whereas $\sigma_{t,max}$ is the maximum tensile stress. The tensile strain at the maximum load is reported as $\varepsilon_{t,max}$. The exploitation ratio, which is the ratio between the maximum resistance of the TRM specimen ($\sigma_{t,max}$) and resistance of the reinforcing fabric, is also reported. Finally, E_2 is the modulus of elasticity evaluated in the post-cracking phase. The coefficient of variation is reported as a percentage in brackets. Stress-strain curves are reported in Fig. 2.

Table 3. Results of tensile tests on TRM coupons

Specimen	$\sigma_{t,1}$ (MPa)	$\sigma_{t,max}$ (MPa)	$\varepsilon_{t,max}$	Expl. ratio (%)	E_2 (GPa)
T_FAK	-	444 (9%)	0.011 (24%)	31.7	47.5
T_MKK	-	370 (10%)	0.009 (15%)	26.4	40.9
T_LIME	134 (17%)	476 (8%)	0.008 (8%)	34.0	47.2
T_CEM	322 (23%)	661 (13%)	0.012 (25%)	47.1	46.8

Stress-strain curves showed the typical tri-linear behavior in the case of LIME and CEM matrices. It can be observed that for TRAAM systems it was not possible to identify the tensile stress at first cracking ($\sigma_{t,1}$). This is due to some microcracks (not visible to the naked eye) already present in the specimens before testing, probably caused by the shrinkage of the AAMs during the curing phase. This phenomenon, also observed in other literature studies [9], will be further investigated through hygrometric shrinkage tests on the AAMs. The failure mode observed always involved the interface between fabric and mortar. After reaching the peak stress, the fabric starts to slip within the mortar. In all cases the specimens showed a pseudo-ductile tensile

behavior. The plateau observed at the end of the stress-strain curves is due to the friction developed between the fabric and the matrix during the slipping. CEM coupons showed the highest tensile strength, followed by LIME, FAK and MKK. This is probably due to the greater mechanical properties of the cement matrix, and the greater adhesion developed at the fabric-to-mortar interface. The exploitation ratio is comprised between 26% and 47%, which is in line with other literature studies [9].

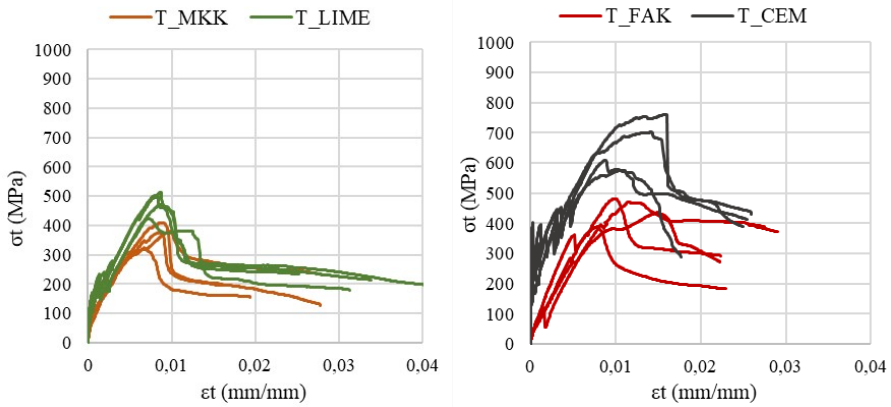

Fig. 2. Stress-strain curves of tensile tests on TRM coupons.

3.3 Single shear bond tests

Single-shear bond tests were performed to evaluate the bond of the mortars to standard red clay bricks (60x120x250 mm^3). Bricks were saturated in water for 24 hours before applying a TRM strip on one side, with a bonded length of 200 mm, width of 60 mm and thickness of about 10 mm. A plastic mold was used to apply the TRM strip on clay bricks (see Fig. 3). Specimens were cured for 28 days at laboratory conditions before testing.

Fig. 3. Preparation of specimens for single-shear bond test.

Shear bond tests were performed with a Zwick Z050 (displacement control at 0.5 mm/min), by restraining the specimen through a steel frame fixed to the base of the testing machine (Fig. 4). GFRP tabs were epoxy bonded at the upper end of the basalt fabric to avoid slippage during the test and to redistribute tensile stresses among the

yarns. Tensile stress was calculated by dividing the tensile load (F) by the cross-sectional area of the fabric. DIC was used to record the fabric displacement (δ) with respect to the clay brick. The coefficient of variation is reported as a percentage in brackets.

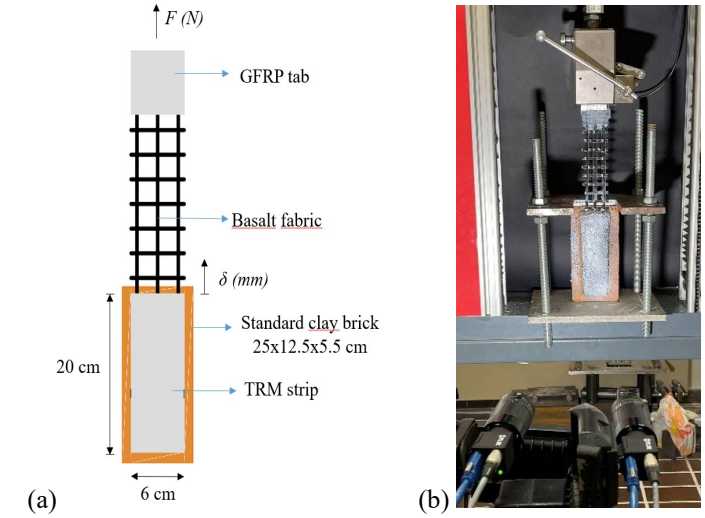

Fig. 4. Single-shear bond test: (a) specimen geometry and (b) test setup.

Results of single-shear bond tests are reported in Table 4, while the experimental load-displacement curves are reported in Fig. 5.

Table 4. Results of single-shear bond tests

Specimen	Peak load F (N)	Stress at peak load (MPa)	Displacement at peak load, δ (mm)	Exploitation ratio (%)
SB_FAK	3243 (10%)	813 (10%)	0.98 (24%)	58.0
SB_MKK	1851 (4%)	464 (4%)	1.49 (8%)	33.1
SB_LIME	2348 (8%)	589 (8%)	1.10 (17%)	42.0
SB_CEM	1556 (16%)	389 (16%)	0.25 (18%)	27.7

FAK, MKK and LIME matrices showed excellent bond with clay brick substrate, since the failure mode observed never involved the interface between mortar and substrate. In these specimens, the failure occurred due to slippage of the basalt fabric within the mortar. The metakaolin-based mortar (MKK) showed a maximum load 20% lower than the commercial lime-based ones (LIME), probably due to the lower mechanical properties of the MKK mortar and the lower bond properties at the fabric-

to-mortar interface. Fly-ash based mortars (FAK) showed excellent bond properties up to a shear load of about 3243 N, corresponding to an exploitation ratio of about 58%. Cement-based mortars showed very poor compatibility with the clay brick substrate, since the failure always involved the interface between mortar and substrate. The specimens failed prematurely, with load values much lower than expected.

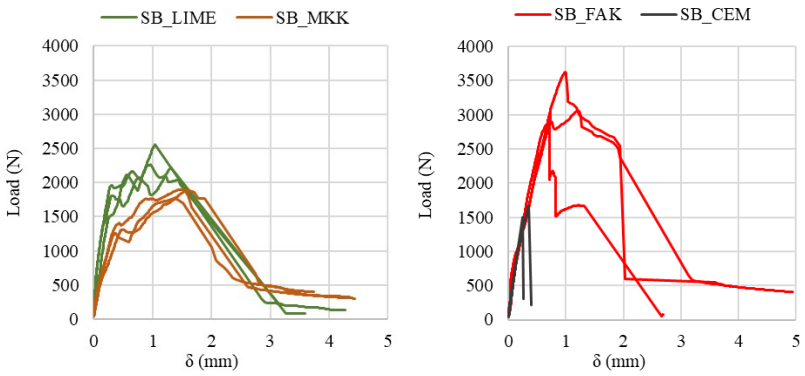

Fig. 5. Shear-bond tests: load-displacement curves.

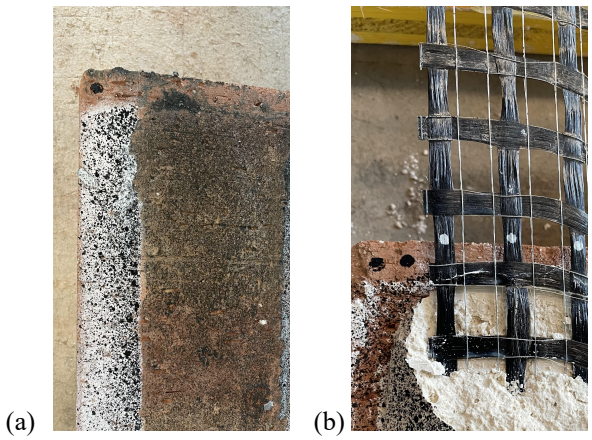

Fig. 6. Failure modes observed: (a) detachment at the mortar-to-substrate interface (CEM), (b) cracking of external layer of the mortar and fabric slippage (FAK, MKK,LIME).

4 Conclusions

In this study the possibility of using alternative AAMs for TRM systems has been preliminary evaluated. The following conclusions can be drawn:

- Both the two investigated AAMs, based on fly ash (FAK) or metakaolin (MKK), proved to be an interesting and sustainable alternative to traditional lime- or cement-based mortars for TRM systems.
- TRAAM systems did not show the typical tensile bi-linear behavior. In particular, the transition point of the first crack is not observed. This is probably due to the shrinkage of AAMs, which caused premature cracking and reduced the adhesion at the fiber-matrix interface. Pseudo-ductile behavior is observed for all specimens, with slippage of the fabric within the mortar.
- The cement-based TRM showed the highest tensile strength, probably due to the greater strength of the matrix and the better adhesion at the fiber-matrix interface.
- On the other hand, AAMs showed great adhesion to clay brick substrates. Failure observed in single-shear tests never occurred at the matrix-substrate interface but rather at the matrix-fiber interface. FAK specimens showed the greatest bond properties, while CEM failed due to debonding at the matrix-to-substrate interface.
- Performances of TRAAM systems can be further improved, for example by optimizing AAMs formulation to reduce shrinkage and by developing new fiber coatings, more compatible with these types of mortars.

References

1. Koutas LN, Tetta Z, Bournas DA, Triantafillou TC. Strengthening of Concrete Structures with Textile Reinforced Mortars: State-of-the-Art Review. Journal of Composites for Construction. 2019; 23(1): 03118001.
2. Donnini J, Corinaldesi V. Mechanical characterization of different FRCM systems for structural reinforcement. Constr Build Mater. 2017; 145: 565-575.
3. Donnini J, Bompadre F, Corinaldesi V. Tensile behavior of a glass FRCM system after different environmental exposures. Processes. 2020; 8(9), 1074.
4. Mobili A, Belli A, Giosuè C, Bellezze T, Tittarelli F. Metakaolin and fly ash alkali-activated mortars compared with cementitious mortars at the same strength class. Cement and Concrete Research. 2016; 88: 198-210.
5. Tempest B, Sanusi O, Gergely J, Ogunro V, Weggel D. Compressive strength and embodied energy optimization of fly ash based geopolymer concrete. 3rd World of Coal Ash, WOCA Conference – Proceedings. 2009.
6. Tang W, Pignatta G, Sepasgozar S, Life-cycle assessment of fly ash and cenosphere-based geopolymer material. Sustainability. 2021; 13(20): 11167.
7. He R, Dai N, Wang Z. Thermal and Mechanical Properties of Geopolymers Exposed to High Temperature: A Literature Review. Adv Civ Eng. 2020: 7532703.
8. Pacheco-Torgal F, Abdollahnejad Z, Camões AF, Jamshidi M, Ding Y. Durability of alkali-activated binders: A clear advantage over Portland cement or an unproven issue? Constr Build Mater. 2012; 30: 400–405.
9. Arce A, Azdejkovic L, Miranda de Lima L, Papanicolaou CG, Triantafillou TC. Mechanical behavior of textile reinforced alkali-activated mortar based on fly ash, metakaolin and ladle furnace slag. Open Research Europe. 2022; 2: 79.
10. Arce A, Kapsalis P, Papanicolaou CG, Triantafillou TC. Diagonal Compression Tests on Unfired and Fired Masonry Wallettes Retrofitted with Textile-Reinforced Alkali-Activated Mortar. Journal of Composites Science. 2024; 8(1): 14.